Fuel 90 (2011) 2359–2366

Contents lists available at ScienceDirect

Fuel

journal homepage: www.elsevier.com/locate/fuel

# Mechanistic investigation of chemical looping combustion of coal with $Fe_2O_3$ oxygen carrier

Baowen Wang [a], Rong Yan [b,c,*], Ying Zheng [a], Haibo Zhao [a], Chuguang Zheng [a]

[a] State Key Laboratory of Coal Combustion, Huazhong University of Science and Technology, Wuhan 430074, PR China
[b] School of Material Science and Engineering, Nanyang Technological University, Block N4.1, Nanyang Avenue, Singapore 639798, Singapore
[c] Institute of Environmental Science and Engineering, Nanyang Technological University, Innovation Center, Block 2, Unit 237, 18 Nanyang Drive, Singapore 637723, Singapore

ARTICLE INFO

*Article history:*
Received 14 January 2010
Received in revised form 23 December 2010
Accepted 8 March 2011
Available online 21 March 2011

*Keywords:*
Chemical looping combustion
Coal
$Fe_2O_3$ oxygen carrier
TGA
Mechanistic study

ABSTRACT

The reaction of three Chinese coals with $Fe_2O_3$ oxygen carrier (OC) was performed in a thermogravimetric analyzer (TGA), with special focuses on the effects of varying heating rate and coal rank on reactivity. Fourier transform infrared spectroscopy (FTIR) was used to in situ detect the emitted gases from TGA. Field scanning electron microscopy/energy-dispersive X-ray spectrometry (FSEM–EDX) was used to study the morphology and elemental compositions of the reaction residues collected from TGA and the related phase evaluation was further identified by X-ray diffraction (XRD). Through all these experiments, it was found that the pyrolysis of coal samples without $Fe_2O_3$ OC under $N_2$ atmosphere underwent the dehydration and the ensuing primary and secondary pyrolysis stages. The increasing heating rate shifted the characteristic temperature ($T_m$) of the primary pyrolysis to a higher temperature and favored a more rapid generation of volatile matters. When the three coals reacting with $Fe_2O_3$ OC, TGA results demonstrated even over 200 °C, the reaction still experienced the partial pyrolysis at the relatively low temperature and the ensuing two reactions of $Fe_2O_3$ with the pyrolysis products at the primary and secondary stages. The coal of low rank with high volatile content should be preferred for the full conversion of coal into $CO_2$. Furthermore, the activation energy of $Fe_2O_3$ OC reacting with PDS at its primary pyrolysis stage was the largest, more than 70 kJ/mol. Finally, SEM–EDX and further XRD analysis of the residues from the reaction of PDS with $Fe_2O_3$ OC indicated the reduced counterpart of $Fe_2O_3$ was $Fe_3O_4$, and some inert iron compounds such as $Fe_2SiO_4$ and $FeAl_2O_4$ were also generated, which might deteriorate the reactivity of $Fe_2O_3$ OC.



## 1. Introduction

The large consumption of fossil fuels, especially coal, has been recognized as one of the main anthropogenic sources of $CO_2$ emission into the atmosphere, which exerts great concerns such as detrimental greenhouse effect and global warming. Actions to capture $CO_2$ from fossil fuel combustion are therefore of great necessity. Among all the available techniques of carbon capture, chemical looping combustion (CLC) is promising for its distinguishable advantage with the inherent separation of $CO_2$ which does not require any extra gas separation unit [1]. Most of past CLC researches are considering gas fuels (such as natural gas and syngas etc.), using solid fuel (i.e. coal) in CLC application would be more beneficial in view of carbon reduction thus is attracting researchers' interests.

There are two routes in applying coal in CLC, the first is to use the syngas derived from coal gasification as the fuel, and the other is to directly introduce coal particles into the CLC system. The latter route would apparently be more economically favorable as it doesn't need the energy-intensive gasification of coal [2]. Leion et al. [3] investigated the direct use of coal from different sources in CLC in a laboratory fluidized bed reactor. Berguerand and Lyngfelt [4] designed a 10 kWth fluidized pilot reacting with a South African coal as the fuel, and Shen et al. [5] also started a CLC application with a Chinese coal on a spouted fluidized system with the same capacity. All these previous works demonstrated initially the feasibility of direct use of coal for CLC application. Also, they have uncovered that the dominant rate-determining step involved in the reaction of coal with OC was actually the coal gasification, instead of the reduction of OC with the gasification products generated in situ from the coal inside the CLC system [3–5]. It was also revealed that in relative to those metal oxides with even higher reactivity (such as NiO and CuO), the $Fe_2O_3$ OC was active enough for reacting with coal efficiently in CLC.

In order to improve the coal gasification in the coal-based CLC system and therefore to fully convert coal to $CO_2$ at a high efficiency facilitating the downstream sequestration, it is necessary

* Corresponding author at: School of Material Science and Engineering, Nanyang Technological University, Block N4.1, Nanyang Avenue, Singapore 639798, Singapore. Tel.: +65 67943244; fax: +65 67921291.
*E-mail address:* ryan@ntu.edu.sg (R. Yan).

0016-2361/$ - see front matter © 2011 Elsevier Ltd. All rights reserved.
doi:10.1016/j.fuel.2011.03.009

to conduct an in-depth investigation on coal gasification with the presence of OC under well manipulated conditions to better understand the mechanism involved. To this end, using TGA, Cao et al. [6] investigated the reduction of CuO with a sub-bituminous coal, Zhao et al. [7] experimented the sol–gel-derived NiO based OC with a Chinese coal char, and Siriwardane et al. [8] attempted to study the reaction of a US coal with various metal oxides. However, due to the complexity of coal gasification in CLC with various thermo-chemical phenomena, the reduction mechanism of OC by coal and their kinetics in CLC system remain unclear.

In addition, after the full conversion of coal with OC, the effective separation of the reduced OC from coal ash is critical and should be properly addressed [2]. The interaction between the reduced OC and ash components would form some inert compounds, which might cause adverse effects, such as decreasing the content of active metal oxides present in OC and thus deteriorating the reactivity, lowering the melting point of the formed ash and possibly causing agglomeration of the reduced OC with ash [8,9]. These would suggest the potentially great difficulty in separating the reduced OC from the formed coal ash. Therefore, further researches are worthy to understand the effect of ash deposit on OC and reveal the possible interaction pathways involved under different CLC process conditions.

In this study, the reduction of $Fe_2O_3$ OC with three Chinese coals of different ranks was investigated using TGA, with focuses on the effect of heating rate and coal rank. FTIR coupled with TGA was used to characterize the emitted gases. The morphology and chemical properties of the reduced OC products were characterized using FSEM coupled with EDX, and their phases were further identified by XRD. This study could provide useful information for establishing a practical coal-based CLC system through a better understanding to the mechanisms associated.

## 2. Experimental procedures

### 2.1. Materials and characterization

Three Chinese coals of different ranks were selected, including Ping Ding Shan bituminous coal, Liu Pan Shui lean coal and Yang Quang anthracite, hereafter designed as PDS, LPS and YQ, respectively. The original coal samples were firstly dried at 105 °C for 24 h to remove the containing moisture, and then ground and sieved to collect the samples in 63–106 μm for the ensuing use. The proximate and ultimate analyses of the three prepared coal samples are presented in Table 1. It was found that with the enhanced rank of three coals from PDS to LPS and to YQ, the content of volatile and the ratio of H to C descended whilst the content of fixed carbon increased. The ash contents of three coals were increased from 24.9% to 29.2% and contrarily the heating value (LHV) decreased from 27.5 to 22.7 MJ/kg, with the increase of coal rank.

Furthermore, three coal ashes were produced through heating at 30 °C/min in a muffle furnace from the ambient up to 815 °C and holding the temperature for 2 h, until the weight of the ashed samples was stabilized. The ash components of three coals were tested using X-ray fluorescence (XRF, Philips, PW 2400, Netherlands) and the results are summarized in Table 2. Compounds containing Si, Al and Fe were observed to be the three major components and their total content made up more than 80 wt.% in all the three coal ashes.

Besides coal samples, the $Fe_2O_3$ OC used (including $Fe_2O_3$ alone and $Fe_2O_3$ with support $Al_2O_3$ at the mass ratio of 8–2) was synthesized by the novel sol–gel combustion synthesis (SGCS) method, using hydrated nitrates and urea as the precursors. The procedure of SGCS was briefly iterated hereafter. Firstly, the stoichiometric compositions of metal nitrates (including nitrates of iron and aluminium) and urea were calculated, and then the accurately weighted nitrates and urea were dissolved in DI water sequentially. The mixture was then stirred on a hot plate under the air atmosphere and aged at 75 °C until the formation of viscous colloidal. Following that, the wet sol was dried at ~135 °C in a desiccator overnight, and then transferred into a ceramic dish and ignited in the preheated muffle furnace at 600 °C for 15 min. Finally, the as-ignited product proceeded to be sintered in the same furnace at 950 °C for 2 h. The more detailed procedure and the characterization of the formed oxides were elaborated elsewhere [10]. Similarly, after grinding and sieving, the oxides in 63–106 μm were used. Finally, the as-prepared coals were evenly mixed with the synthesized $Fe_2O_3$ OC at the designed mass ratio (as seen in Section 2.2) in a laboratory mortar.

### 2.2. Determination of oxygen excess number $\phi$ for different coal samples

The full conversion of coal is determined by the availability of oxygen present in OC. Sufficient but not over supply of the OC is very important to operate the CLC system economically. Hereafter, the method of coal mass balance was adopted to determine the amount of $Fe_2O_3$ OC to be inputted into the CLC system. Similar to the reference [16], from the proximate and ultimate analysis results, the weight fractions of hydrogen and oxygen in the moisture were deducted and thus the remaining free hydrogen and oxygen could be determined. If 1 kg of coal samples were used, the content of different atoms (including C, H, O, N, S) contained in the coal samples could be determined and the relative chemical formula was represented as $C_\alpha H_\beta S_\gamma O_\delta (N_2)_\nu$. Finally, for $Fe_2O_3$ OC, supposing the reduced counterpart was $Fe_3O_4$ when coal being fully converted, the reduced reaction of $Fe_2O_3$ OC with different coal samples could be depicted below:

$$C_\alpha H_\beta S_\gamma O_\delta (N_2)_\nu + 3\ (2\alpha + \beta/2 + 2\gamma - \delta)Fe_2O_3 \rightarrow 2(2\alpha + \beta/2 + 2\gamma - \delta)Fe_3O_4 + \alpha CO_2(g) + \beta/2 H_2O(g) + \gamma SO_2(g) + \nu N_2(g) \quad (1)$$

From Eq. (1), the theoretic stoichiometric oxygen needed for the full conversion of coal is $3(2\alpha + \beta/2 + 2\gamma - \delta)$, and supposing the realistic

**Table 1**
Proximate and ultimate analysis of the coal samples.

| Samples | Proximate analysis[a] (wt.%) | | | | Ultimate analysis (wt.%, $d$[b]) | | | | | LHV[d] (MJ/kg) |
|---|---|---|---|---|---|---|---|---|---|---|
| | $M_{ad}$ | $V_{ad}$ | $A_d$ | $FC_{ad}$ | C | H | N | S | O[c] | |
| PDS | 1.11 | 29.18 | 24.92 | 44.79 | 56.77 | 2.87 | 2.74 | 0.56 | 37.06 | 27.53 |
| LPS | 3.09 | 22.84 | 25.38 | 48.69 | 62.89 | 2.31 | 1.27 | 0.89 | 32.64 | 23.49 |
| YQ | 2.39 | 8.05 | 29.24 | 60.32 | 64.02 | 1.81 | 1.1 | 0.67 | 32.4 | 22.71 |

[a] $M$: moisture content; $V$: volatile matters; $A$: ash content; FC: fixed carbon; ad: air-dried basis.
[b] Dry basis.
[c] The O content was determined by difference.
[d] Low heating value.

**Table 2**
Ash compositions of three coals (wt.%).

| Coal ashes | $SiO_2$ | $Al_2O_3$ | $Fe_2O_3$ | $SO_3$ | CaO | $TiO_2$ | $K_2O$ | MgO | $Na_2O$ |
|---|---|---|---|---|---|---|---|---|---|
| PDS | 59.74 | 20.11 | 9.98 | 3.31 | 2.12 | 1.32 | 0.92 | 0.55 | 0.2 |
| LPS | 41.31 | 24.07 | 17.0 | 4.60 | 3.12 | 2.80 | 1.41 | 1.58 | 0.62 |
| YQ | 68.49 | 14.58 | 4.48 | 4.10 | 3.65 | 0.69 | 1.04 | 0.63 | 1.24 |

oxygen contained in OC was Y(O), then the oxygen excess number $\phi$ was determined below.

$$\Phi = \mathrm{Y(O)}/(3(2\alpha + \beta/2 + 2\gamma - \delta)) \quad (2)$$

In Eq. (2), $\Phi = 1$ referred that the $Fe_2O_3$ OC supplied theoretically just met the requirement of a full conversion of coal. According to the aforementioned method, the relative chemical formula of PDS, LPS and YQ of 1 kg could be depicted, respectively, as $C_{35.1}H_{20.2}N_{1.45}S_{0.13}O_{16}$, $C_{37.9}H_{14.1}N_{0.66}S_{0.2}O_{13.5}$ and $C_{36.8}H_{10.2}N_{0..54}S_{0.144}O_{13.1}$. Then, based on Eq. (2), if $\Phi = 1$, the mass ratio of $Fe_2O_3$ supplied to PDS, LPS and YQ were correspondingly 38.2, 41.8 and 39.5.

### 2.3. Experimental methods

The reaction characteristics of the synthesized $Fe_2O_3$ OC with three different coals at the oxygen excess number $\phi = 1$ were investigated using TGA (TA 2050, US). The mixture of coal and $Fe_2O_3$ OC was heated from ambient to 150 °C at the heating rate of 10 °C/min and held at the final temperature for up to 10 min so as to fully remove the moisture. Then, it was further heated up to 850 °C at 35 °C/min with holding the final temperature for 10 min to ensure the full conversion of coal. The flow rate of $N_2$ and the total mass for the mixture of coal and OC were determined, respectively, at 50 ml/min and ~15 mg after many pre-screening experiments, to eliminate the potential impact of mass transfer between gas and solid phases.

The evolved gases from the reaction of coal with $Fe_2O_3$ OC in TGA, were firstly dried through a portable tubular gas desiccator fully of $Ca(SO_4)\cdot 2H_2O$, and were then in situ detected by FTIR spectrometer equipped with a deuterated triglycine sulfate (DTGS) detector (BioRad Excalibur Series, model FTS 3000). The FTIR was coupled with TGA 2050. The scanning range of IR was 4000–500 $cm^{-1}$, and the resolution and sensitivity were pre-set at 4 $cm^{-1}$ and 1, respectively.

Finally, the morphology and elemental composition of the reaction products from coal with $Fe_2O_3$ OC were studied using FSEM (Siron 200, Netherlands) coupled with an EDX (GENESIS, US) at a magnification of 800 and an accumulated voltage of 30 kV. The formed phases were further identified by XRD (X'Pert PRO, Netherlands) with 40 kV 40 mA Cu Kα ($\lambda = 0.154$ Å) radiation and the step-scanned range of 10–80°.

### 2.4. Calculation of kinetic parameters

A study on the reaction kinetics is essential to obtain a better insight into the mechanism of coal reacting with $Fe_2O_3$ OC. Assuming that the reaction of coal with $Fe_2O_3$ OC in this study is mainly controlled by the reaction itself and the limitation of mass and heat transfers involved are negligible at the current experimental conditions. The popular Coats and Redfern method was applied to determine the kinetic parameters for coal reacting with $Fe_2O_3$ OC based on the recorded data from TGA. The detailed expressions, used to calculate the related kinetic parameters, were iterated below.

$$\ln[F(\alpha)] = -(E/RT) + \ln(AR/\beta E) \quad (3)$$

$$F(\alpha) = -(1-\alpha)/T^2 \quad (\text{for } n = 1) \quad (4)$$

$$F(\alpha) = -1 - (1-\alpha)^{1-n}/(1-n)T^2 \quad (\text{for } n \neq 1, \quad n = 0, 0.5, 1.5, 2\ldots) \quad (5)$$

where $\beta$ is the heating rate used, $\beta = dT/dt$, $T$ (K) and $t$ (s) are correspondingly referred to temperature and time. The conversion fraction $\alpha$ is given as $\alpha = (W_0 - W)/(W_0 - W_\infty)$, in which $W$ is the mass of the solid sample and the subscripts of "0" and "$\infty$" denote the initial and final residual mass left for the reaction of coal with $Fe_2O_3$ OC, respectively. Kinetic parameters of $E$ (kJ/mol) and $A$ (1/s) represent the activation energy and the pre-exponential factor. $R$ is the general gas constant (J/mol K) and $n$ is the reaction order.

## 3. Results and discussion

### 3.1. Baseline experiment of coal pyrolysis without $Fe_2O_3$ OC

In order to gain an in-depth understanding to the reaction characteristics of coal in CLC, first as a basis, the pyrolysis of three Chinese coals (PDS, LPS and YQ) without the presence of $Fe_2O_3$ were performed in TGA under $N_2$ atmosphere, with special focuses on the effect of different heating rates (10 and 35 °C/min). The results of mass loss (i.e., TG curve) are depicted in Fig. 1a, and those of differential mass loss rate (i.e., DTG curve) are shown in Fig. 1b and c for the heating rate of 10 and 35 °C/min, respectively.

Firstly, from Fig. 1a and b, taking PDS coal as an example, at the heating rate of 10 °C/min, it could be observed that the pyrolysis of PDS mainly occurred around 200–800 °C. After the dehydration occurred at below 200 °C, PDS mainly underwent two distinct pyrolysis stages, including primary pyrolysis and the ensuing secondary pyrolysis, of which the first one fell into 200–680 °C with the characteristic temperature $T_m$ (i.e., DTG peak temperature) centering at 476 °C, and emitted approximately 25 wt.% of volatile matter, mainly consisting of $CH_4$, $C_2H_6$, $CO_2$, $H_2O$, etc., as evidenced in Fig. 3, and the corresponding mass loss rate reached 1.7 wt.%/min. After the primary pyrolysis of PDS, another lower weight loss, almost indiscernible, occurred higher than 680 °C, with around 2.8 wt.%/min emitted, resulting from the cleavage and condensation of the main carbon matrix [11].

The effect of coal rank was analyzed from the behaviors of three coal samples of different ranks. Similar to the pyrolysis characteristics of PDS, both LPS and YQ also demonstrated two different pyrolysis stages (see Fig. 1b) at above 200 °C, but their peak mass loss rate for the primary pyrolysis decreased rapidly from 1.7 wt.%/min of PDS to 0.27 wt.%/min of YQ, with the enhanced coal rank. On the contrary, the peak mass loss rate of the secondary pyrolysis of YQ (0.46 wt.%/min) was even more significant compared to those of PDS and LPS, due to possibly the much higher fixed carbon content in YQ with the increase of coal rank. Furthermore, in Fig. 1a, after the pyrolysis, the emitted weight fraction of the three coals decreased with the enhanced coal rank, similar to the previous report [12]. Meanwhile, in Fig. 1b, it was found that the characteristics temperature $T_m$ in both pyrolysis stages was shifted towards a higher value with the increase of coal rank, similar to the finding of Burnham et al. [13].

Heating rate also showed a significant influence on the coal pyrolysis. Compare Fig. 1c and b, it could be found that with the increase of heating rate from 10 to 35 °C/min, the peak mass loss rate of three coals greatly increased (note the different scales of mass loss rate). Especially for PDS at the primary pyrolysis stage, it was increased from 1.7 to 5.8 wt.%/min. Furthermore, though the similar increasing trend of peak mass loss rate was found for LPS and YQ, the degree of increase was descended with the enhanced rank of coal. Meanwhile, the characteristic temperatures of all three coals were found to shift to a higher temperature with the enhanced heating rate, mainly due to the retardancy of the

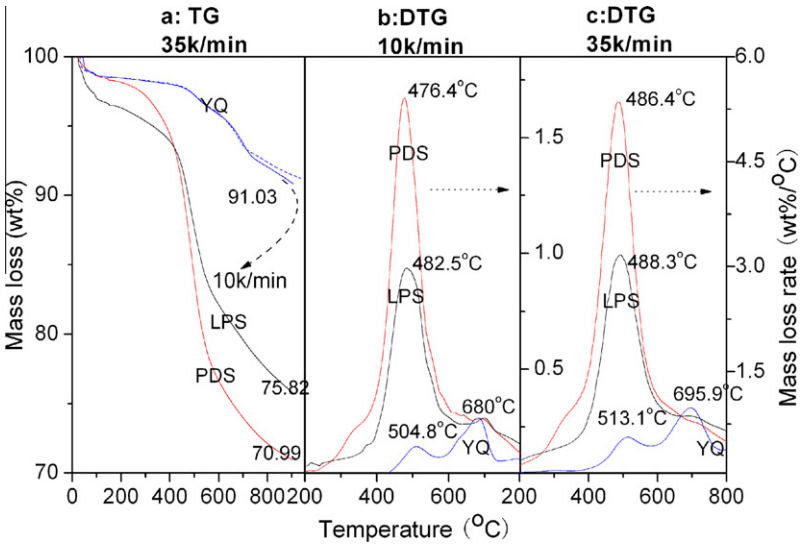


**Fig. 1.** Effect of the heating rate on the pyrolysis of three coals under $N_2$ atmosphere.

diffusion of volatile matters and heat transfer [14]. Overall, the heating rate increase benefited the pyrolysis of coal of all ranks and promoted the fast evolving of volatile matters in coal [15], especially for coal at low rank.

### 3.2. Investigation of the reduction of $Fe_2O_3$ OC with three coal samples

#### 3.2.1. TGA–FTIR analysis of the reduction of $Fe_2O_3$ OC by different coals

The reactions of three coals with $Fe_2O_3$ OC at the oxygen excess number $\Phi = 1$ under $N_2$ atmosphere were performed in TGA. The heating rate of 35 °C/min was chosen. The temperature was increased to 850 °C with an isothermal period of 10 min for a full reaction of coal. The results are shown in Fig. 2a and Fig. 2b, with *X*-axis in time instead of temperature. Meanwhile, the inert support of OC (such as $Al_2O_3$) is also necessary for improving the resistance to sintering, abrasion and fragmentation over cyclic reactions in the CLC system. The reactions between three coals and $Fe_2O_3$/$Al_2O_3$ were also investigated and the related results are depicted in Fig. 2c.

Firstly, from Fig. 2a, in the range of 200–850 °C, PDS reacted more easily with $Fe_2O_3$ with a higher weight loss (2.5 wt.%) than other two coals of higher rank, especially for YQ with weight loss less than 1.0 wt.%. But the final weight losses for the reaction of different coal samples with $Fe_2O_3$/$Al_2O_3$ oxygen carrier were found to be less than those corresponding losses for the reaction of coal with $Fe_2O_3$ only, due to the introduction of the support $Al_2O_3$, which was inert to coal. In Fig. 2b, three reaction stages were observed from the DTG curves, different from the cases of without $Fe_2O_3$ as shown in Fig. 1c. Similar finding of three-staged reaction was reported by Siriwardane et al. [8]. For PDS, the corresponding three characteristic temperatures were respectively at 496, 619 and 810 °C. The first reaction was most likely related to the partial pyrolysis of PDS in its mixture with $Fe_2O_3$, at the mass loss rate of 0.1682 wt.%/min. Note this value (0.1682 wt.%/min) was much lower than the pyrolysis rate (5.8 wt.%/min) seen for PDS at ~484 °C in Fig. 1c, but if multiplied by 38.2 (the mass ratio of $Fe_2O_3$ to PDS at the oxygen excess number $\Phi = 1$), the calculated mass loss rate of 6.4 wt.%/min was reasonable. The ensuing two reactions happened at 619 and 810 °C in Fig. 2b would be

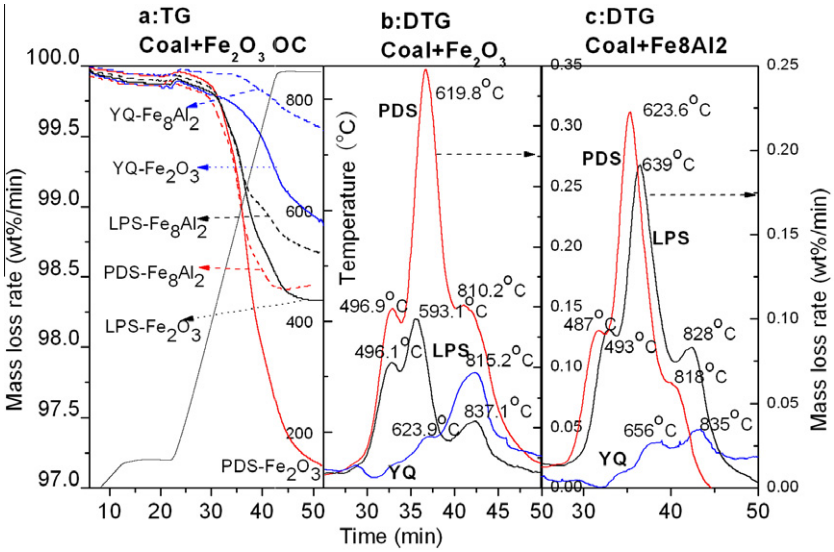


**Fig. 2.** Effect of $Fe_2O_3$ OC on the pyrolysis of various coals under $N_2$ atmosphere.

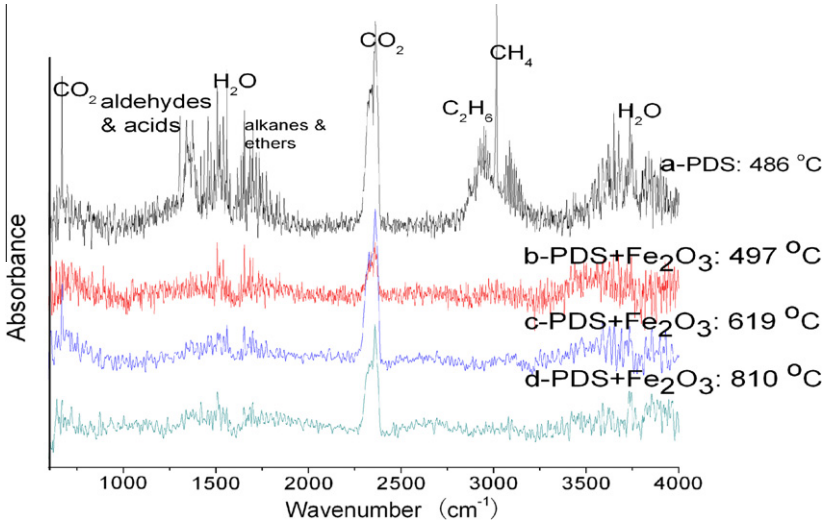


**Fig. 3.** FTIR spectra of gas products from the reaction of PDS coal with $Fe_2O_3$ OC.

identified as the reaction of PDS coal with $Fe_2O_3$ through its primary and secondary pyrolysis. Such assumption could be further validated by the evolved gas products from the reaction of PDS with $Fe_2O_3$, which was identified by FTIR analysis at different reaction stages, and the result is shown in Fig. 3. The only major gas product was $CO_2$ at 619 and 810 °C from the reaction of PDS coal with $Fe_2O_3$ for two-stage pyrolysis, indicating the full conversion of coal. It is noteworthy that the peak temperature 619 °C (the first PDS reaction with $Fe_2O_3$) was 350 °C lower than the data reported by Siriwardane et al. where a Illinos #6 coal reaction with commercial $Fe_2O_3$ was considered [8]. The big temperature discrepancy was expected to mainly arise from the reactivity difference of the two $Fe_2O_3$ samples used whilst the latter was synthesized by the home designed method.

Analyzing the effect of coal rank, from Fig. 2b, all the three coals demonstrated three stage reactions, but with the increase of coal rank, the corresponding characteristic temperature $T_m$ were found to shift to higher values, the same trend as observed for coal pyrolysis alone in Fig. 1c. This indicated that coal of higher rank reacted with $Fe_2O_3$ more difficulty [17]. In view of applying $Fe_2O_3$ OC in a coal-based CLC system, the coal of low rank with high volatile matters would be preferred. Finally, in Fig. 2c, the effect of inert support $Al_2O_3$ on the reaction of coal with $Fe_2O_3$ was shown. The mass ratio of $Fe_2O_3$ to $Al_2O_3$ was 8–2. Similarly three reaction stages occurred and the corresponding characteristic temperatures increased with the enhanced coal rank.

### 3.2.2. Kinetic analysis

In order to gain a better understanding to the reaction of three coals with $Fe_2O_3$ OC, the relevant kinetic parameters, including activation energy $E$ and pre-exponent $A$, were calculated by Eqs. (3)–(5). PDS was more selective to $Fe_2O_3$ OC and thus adopted as a representative. The TGA data obtained from Figs. 1c and 2 at the heating rate of 35 °C/min are selected and the calculated results are shown in Table 3.

From this table, all the correlation coefficients (CR) for the related kinetic parameters were larger than 0.99 with one exception for the reaction of PDS with $Fe_2O_3/Al_2O_3$. In relative to the activation energy $E$ = 44.9 kJ/mol for the pyrolysis of PDS at 200–840 °C, with the inclusion of $Fe_2O_3$ and $Fe_2O_3/Al_2O_3$ OC the $E$ values of PDS pyrolysis at 220–530 °C decreased first slightly to 43.8 and 40.1 kJ/mol, respectively, indicating the catalytic effect of OC to coal pyrolysis. However, at 500–780 °C, the $E$ values increased a lot to 73.6 kJ/mol and to 96.1 kJ/mol for the reactions of PDS with $Fe_2O_3$ and $Fe_2O_3/Al_2O_3$, respectively. Furthermore, at 780–850 °C, the related reaction activation energy $E$ for both reactions of PDS with $Fe_2O_3$ and $Fe_2O_3/Al_2O_3$ decreased to below 70 kJ/mol, possibly because the products of secondary pyrolysis of coal contained a large fraction of $H_2$ and CO [11], which more easily reacted with $Fe_2O_3$ OC than those from the primary pyrolysis stage.

**Table 3**
Kinetics parameters of PDS coal with $Fe_2O_3$ OC under $N_2$ atmosphere at the heating rate of 35 °C/min.

| Samples | Temperature (°C) | $n$ | $E$ (kJ/mol) | $A$ (1/s) | −CR[a] |
|---|---|---|---|---|---|
| PDS | 200–840 | 2 | 44.9 | 53.5 | 0.9971 |
| PDS + $Fe_2O_3$ | 220–530 | 2 | 43.8 | 3.7 | 0.9981 |
| | 530–750 | 2 | 73.6 | 726.9 | 0.9996 |
| | 750–840 | 2 | 59.4 | 90.4 | 0.9945 |
| PDS + $Fe_2O_3/Al_2O_3$ | 370–540 | 2 | 40.1 | 0.92 | 0.9947 |
| | 540–780 | 2 | 96.1 | 7191.4 | 0.9969 |
| | 780–845 | 2 | 67.5 | 5372.1 | 0.9839 |

[a] Correlated coefficient.

### 3.3. Chemical and microstructure analysis

To help understand the issue of ash separation from the reaction of coal with OC, the morphology and elemental composition of both residues from PDS coal pyrolysis, and its reaction with $Fe_2O_3$ OC and $Fe_2O_3/Al_2O_3$ (mass ratio 8:2) were characterized using SEM–EDX. The results are shown in Fig. 4a-c, respectively.

In Fig. 4a for the pyrolysis of PDS, it could be observed in SEM pattern that the residue of PDS consisted of the fragmentary white discrete particle as shown in the spot 1 and the relatively dark bulk shown in spot 2. By the EDX analysis, the elemental composition of the spot 1 was identified as minerals, mainly composed of Si, Al, O and C. For the spot 2, it was possibly the carbon matrix left after PDS pyrolysis with the atomic fraction of C reached 81.71%, which was much higher than that presented in the spot 1 (32.0% of atomic fraction). The presence of Al, Si and S might be resulted from the minerals occurring inherently in the carbon matrix. Furthermore, as shown in Fig. 5a, XRD analysis of the residue from PDS pyrolysis indicated that $SiO_2$ and some silicates, such as $Fe_2Si_2O_5(OH)_4$, $Al_2Si_2O_5(OH)_4$ and $CaAl_2Si_2O_8.4H_2O$, were the main mineralogy compositions. Although the most part of residue should be ascribed

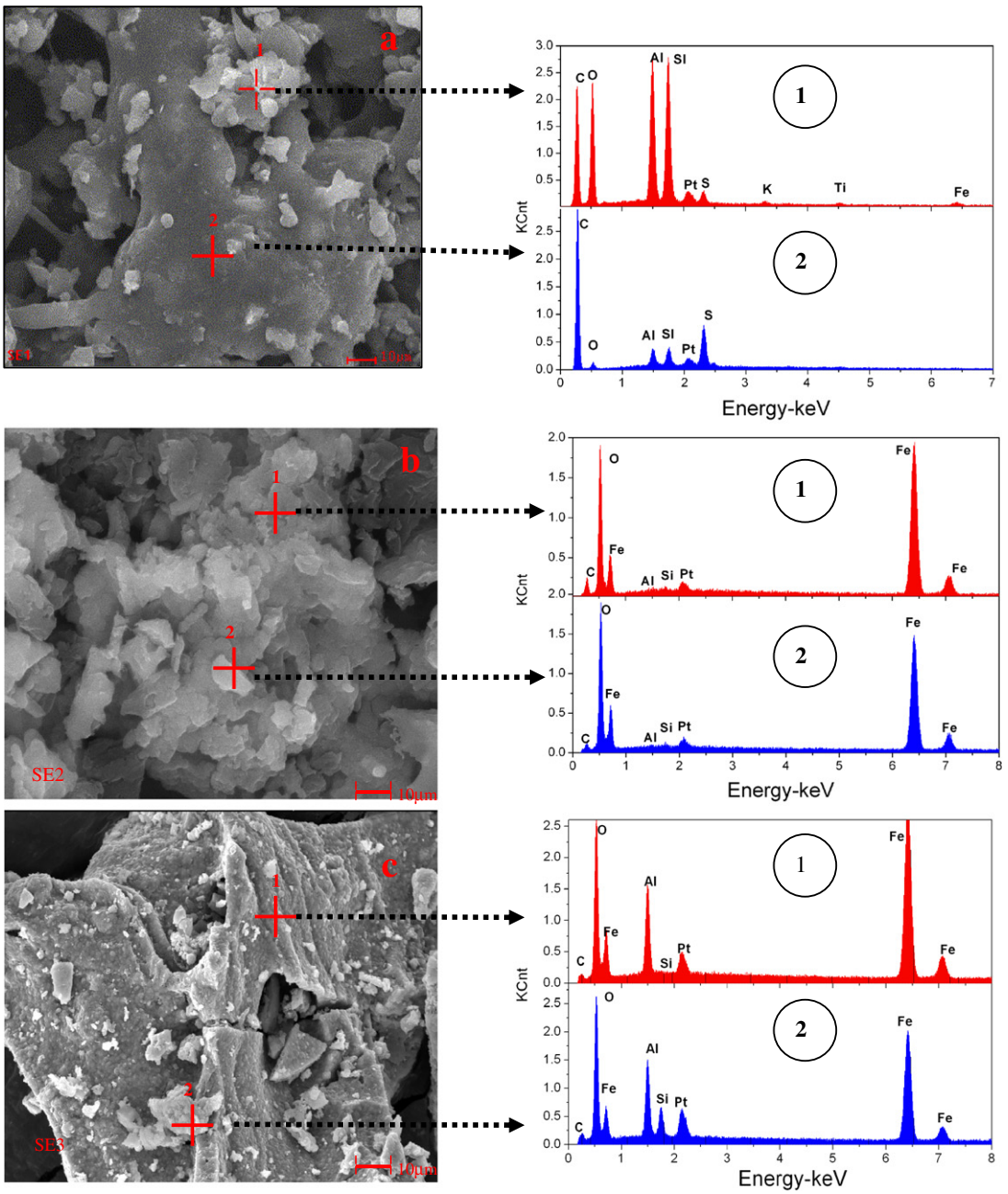


**Fig. 4.** SEM-EDX analysis of the PDS coal pyrolysis (a) and reaction with $Fe_2O_3$ (b) and reaction with $Fe_2O_3/Al_2O_3$ (mass ratio 8:2) (c) (The magnification number was 800 and the accumulated voltage was 30 kV.).

to the carbon matrix by EDX analysis, it cannot be identified in XRD analysis due to its amorphous characteristics.

In Fig. 4b for the reaction of PDS with $Fe_2O_3$, it could be observed in SEM pattern that the reaction residue mainly consisted of discrete white particles, and the two optionally selected spots shown in the SEM pattern were scanned by EDX. It showed that the elemental compositions involved in the two spots were almost the same, which mainly consisted of Fe, O and C, with their atomic fractions equal to 44%, 50% and 5.6%, respectively. The contained iron oxide could be further inferred as $Fe_3O_4$ by the atomic ratio of Fe to O, which could be further validated from the XRD analysis presented in Fig. 5c. The valence of the reduced $Fe_2O_3$ was mainly determined by the mass ratio of $Fe_2O_3$ to carbonaceous material such as biomass [18,19]. When $Fe_2O_3$ OC was used in a CLC system, the potential defluidization of the fuel reactor was observed arising from the reduction of $Fe_2O_3$ further into the lower valence than $Fe_3O_4$ [20]. From this research, if such an undesirable circumstance would be avoided, high mass ratio of $Fe_2O_3$ to coal should be adopted, as suggested by Eq. (2).

Furthermore, to understand the role of inert support, the solid residues from the reaction of $Fe_2O_3/Al_2O_3$ with PDS were further investigated with FSEM–EDX, as shown in Fig. 4c. No sintering phenomenon was found due to the high resistance to sintering of $Al_2O_3$. The atomic fraction of C was ~3%, much less than the case of PDS reaction with $Fe_2O_3$, shown in Fig. 4b, which proved that the presence of $Al_2O_3$ improved the reactivity of $Fe_2O_3$ based OC and promoted the conversion of PDS. Meanwhile, although the Al compositions on the two spots were evenly distributed, with atomic fractions approaching ~15%, but the distribution of Si compositions on the two spots differed greatly, as such, the detailed phases

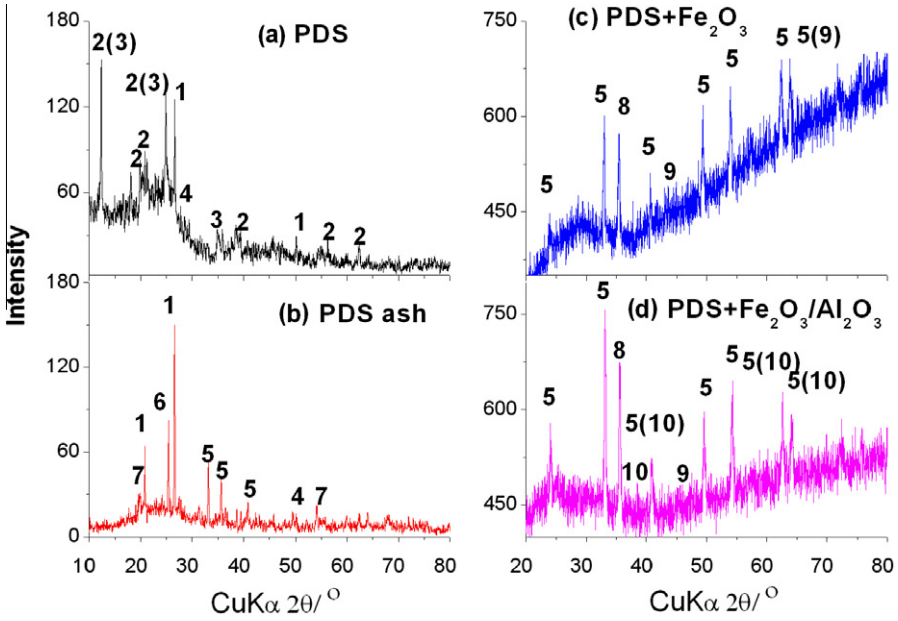


**Fig. 5.** XRD study of the PDS coal with $Fe_2O_3$ OC. In this Fig. 1: quartz [$SiO_2$]; 2: kaolinite [$Al_2Si_2O_5(OH)_4$]; 3: chamosite [ $Fe_2Si_2O_5(OH)_4$]; 4: gismondine[$CaAl_2Si_2O_8.4H_2O$]; 5: hematite [$Fe_2O_3$]; 6: aluminum titanium silicate [$Al_4Ti_2SiO_{12}$]; 7: aluminum calcium silicate [$CaAl_2Si_2O_8$]; 8: magnetite [$Fe_3O_4$]; 9: iron silicate [$Fe_2SiO_4$]; 10: iron aluminum oxide [$FeAl_2O_4$].

of residues from the reaction of PDS with $Fe_2O_3/Al_2O_3$ were further identified with XRD.

Finally, in order to identify the detailed phases involved after the reaction of PDS with $Fe_2O_3$ or $Fe_2O_3/Al_2O_3$, the residues left were identified by XRD, as presented in Fig. 5c and d. From Fig. 5c, after the reaction of $Fe_2O_3$ with PDS, the residue was mainly composed of $Fe_2O_3$, $Fe_3O_4$ and $Fe_2SiO_4$. The $Fe_2O_3$ left mainly resulted from the partial pyrolysis of PDS early at the pyrolysis characteristic temperature of 496 °C as shown in Fig. 2b and the pyrolysis products could not react further with $Fe_2O_3$ at such a low temperature. Of course, such circumstance would not occur in the real CLC system. The presence of $Fe_2SiO_4$ was closely attributed to the interaction of the reduced iron oxide with $SiO_2$ occurred inherently in the coal, especially in the local reducing atmosphere. Similar phase of $Ni_2SiO_4$ was found to occur in the reaction of NiO OC with coal char in our previous experiments [7].

While in Fig. 5d, for the reaction of PDS with $Fe_2O_3/Al_2O_3$ (mass ratio of Fe/Al at 8/2), the residue after reaction mainly consisted of $Fe_2O_3$, $Fe_3O_4$ and $FeAl_2O_4$. The left $Fe_2O_3$ was also owe to the partial pyrolysis of PDS at 487 °C prior to the initiation of PDS reacting with $Fe_2O_3$. The $FeAl_2O_4$ was resulted from the interaction of the reduced iron oxide with $Al_2O_3$, which was included in the $Fe_2O_3/Al_2O_3$ OC [21]. But here $Fe_2SiO_4$ inherent was not identified in the XRD pattern, likely because the reduced iron oxide reacted more easily with $Al_2O_3$ instead of $SiO_2$. At the possible reaction temperature (~850 °C), the reaction enthalpy of the reduced iron oxide with $Al_2O_3$ was -14 kJ, far less than that of the reduced oxide with $SiO_2$ (i.e., −4 kJ). In addition, the identified phases by XRD for the PDS ashing sample (see Fig. 5b) contained $SiO_2$, $Fe_2O_3$, $Al_4Ti_2SiO_{12}$ and $CaAl_2Si_2O_8$, several silicates were observed.

Of course, more attention should be paid to the inert iron compounds such as $Fe_2SiO_4$ and $FeAl_2O_4$, which were formed from the interactions of the reduced iron oxide with $SiO_2$ occurring inherently in coal or with $Al_2O_3$ included in the $Fe_2O_3$ OC. These compounds would not only lower the melting point of $Fe_2O_3$ OC, but also deteriorate the reactivity of OC [9]. Thus, further researches on the mechanisms of forming the inert iron compounds and effective separation of coal ash from the reduced OC through density or magnetic differences in the practical CLC system (such as an interconnected fluidized beds system) with a long duration of continuous operation should be performed.

## 4. Conclusions

The reaction of $Fe_2O_3$ OC with three Chinese coals was performed in TGA, with special focuses on the effect of heating rate and coal rank. The evolved gases from the reaction were detected using on-line FTIR. The morphology and elemental compositions of residues after reactions were analyzed by SEM–EDX, and finally the mineral phases from the reaction residues were further identified by XRD. Through all these measures, such conclusions were reached as follows.

(1) As the baseline, through the pyrolysis of the three coal samples of different ranks without $Fe_2O_3$ OC at the two different heating rates (10 and 35 °C/min), it would be found that coal pyrolysis underwent three different stages, related to the dehydration below 200 °C and the ensuing primary and secondary pyrolysis stages. The related charactersitic temperatures $T_m$ at the two pyrolysis stages shifted to a higher value with the enhanced heating rate and coal rank. Overall, the high heating rate but coal of low rank favored to generate a large amount of volatile matter rapidly.

(2) TGA analysis of three coals reacting with $Fe_2O_3$ or $Fe_2O_3/Al_2O_3$ demonstrated that at over 200 °C, the reaction of three coals experienced three stages, ascribed to the partial pyrolysis at the relatively low temperature and the following reaction of $Fe_2O_3$ with the pyrolysis products at the primary and secondary stages. For PDS, rather then the other two coals of higher rank, was preferred for the full conversion of coal into $CO_2$ in the CLC system using $Fe_2O_3$ OC, though $Fe_2O_3$ OC benefited to improve the pyrolysis rate of all the studied coals of different ranks.

(3) The activation energy of $Fe_2O_3$ or $Fe_2O_3/Al_2O_3$ reacting with PDS at its primary pyrolysis stage was the largest among all the reaction stages, i.e., more than 70 kJ/mol.

(4) SEM–EDX and further XRD analysis of the residues from the reaction of PDS with $Fe_2O_3$ or $Fe_2O_3/Al_2O_3$ indicated that the reduced counterpart of $Fe_2O_3$ was $Fe_3O_4$, and some inert iron compounds such as $Fe_2SiO_4$ and $FeAl_2O_4$ were generated, which could lead to the deterioration of $Fe_2O_3$ OC. Further investigations are needed to understand this issue better.

## Acknowledgments

This work is supported by the A*Star SERC Grant of Singapore (SERC 0921380025-M47070019) and National Natural Science Foundation of China (Nos. 50906030 and 50936001). It is also part of the project "Co-control of Pollutants during Solid Fuel Utilization", supported by the Programme of Introducing Talents of Discipline to Universities (¡°111¡ ± project B06019), China.

## References

[1] Jin H, Okamoto T, Ishida M. Development of a novel chemical-looping combustion: synthesis of a solid looping material of $NiO/NiAl_2O_4$. Ind Eng Chem Res 1999;38(1):126–32.
[2] Cao Y, Pan WP. Investigation of chemical looping combustion by solid fuels. 1. Process analysis. Energy Fuels 2006;20(5):1836–44.
[3] Leion H, Mattisson T, Lyngfelt A. Solid fuels in chemical-looping combustion. Int J Greenhouse Gas Control 2008;2(2):180–93.
[4] Berguerand N, Lyngfelt A. Design and operation of a 10 kWth chemical-looping combustor for solid fuels – testing with South African coal. Fuel 2008;87(12):2713–26.
[5] Shen LH, Wu JH, Xiao J. Experiments on chemical looping combustion of coal with a NiO based oxygen carrier. Combust Flame 2009;156(3):721–8.
[6] Cao Y, Casenas B, Pan WP. Investigation of chemical looping combustion by solid fuels. 2. Redox reaction kinetics and product characterization with coal, biomass, and solid waste as solid fuels and CuO as an oxygen carrier. Energy Fuels 2006;20(5):1845–54.
[7] Zhao HB, Liu LM, Wang BW, Xu D, Jiang LL, Zheng CG. Sol–gel-derived $NiO/NiAl_2O_4$ oxygen carriers for chemical-looping combustion by coal char. Energy Fuels 2008;22(2):898–905.
[8] Siriwardane R, Tian HJ, Richards G, Simonyi T, Poston J. Chemical-looping combustion of coal with metal oxide oxygen carriers. Energy Fuels 2009;23(8):3885–92.
[9] Shen LH, Wu JH, Gao ZP, Xiao J. Reactivity deterioration of $NiO/Al_2O_3$ oxygen carrier for chemical looping combustion of coal in a 10 $kW_{th}$ reactor. Combust Flame 2009;156(7):1377–85.
[10] Wang BW, Yan R, Lee DH, Zheng Y, Zhao HB, Zheng CG. Characterization and evaluation of Fe2O3/Al2O3 oxygen carrier prepared by sol-gel combustion synthesis. J Anal Appl Pyrol 2011. doi:10.1016/j.jaap.2011.01.010.
[11] Yang HP, Chen HP, Ju FD, Yan R, Zhang SH. Influence of pressure on coal pyrolysis and char gasification. Energy Fuels 2007;21(6):3165–70.
[12] Alonso MJG, Alvarez D, Borrego AG, Menéndez R, Marbán G. Systematic effects of coal rank and type on the kinetics of coal pyrolysis. Energy Fuels 2001;15(2):413–28.
[13] Burnham AK, Myongsook SO, Crawford RW. Pyrolysis of Argonne preimum coals: activation energy distributions and related chemistry. Energy Fuels 1989;3(1):42–55.
[14] Seebauer V, Peterk J, Staudinger G. Effects of particle size, heating rate and pressure on measurement of pyrolysis kinetics by thermogravimetric analysis. Fuel 1997;76(13):1277–82.
[15] Pang KL, Xiang WG, Zhao CS. Investigation on pyrolysis characteristic of natural coke using thermogravimetric and Fourier-transform infrared method. J Anal Appl Pyrol 2007;80(1):77–84.
[16] Cyprès R, Soudan-Moinet C. Pyrolysis of coal and iron oxdies mixtures. 1. Influence of iron oxides on the pyrolysis of coal. Fuel 1980;59(1):48–54.
[17] Cyprès R, Soudan-Moinet C. Pyrolysis of coal and iron oxdies mixtures. 2. Reduction of iron oxdies. Fuel 1981;60(1):33–9.
[18] Liu GS, Strezov V, Lucas JA, Wibberley LJ. Thermal investigations of direct iron ore reduction with coal. Thermochim Acta 2004;410(1–2):133–40.
[19] Strezov V. Iron ore reduction using sawdust: experimental analysis and kinetic modelling. Renew Energy 2006;31(12):1892–905.
[20] Cho P, Mattisson T, Lyngfelt A. Defluidization conditions for fluidized-bed of iron, nickel, and manganese oxide-containing oxygen carriers for chemical-looping combustion. Ind Eng Chem Res 2006;45(3):968–77.
[21] Abad A, Garcia-Labiano F, de Diego LF, Gayán P, Adánez J. Reduction kinetics of Cu-, Ni-, and Fe-based oxygen carriers using syngas ($CO + H_2$) for chemical-looping combustion. Energy Fuels 2007;21(4):1843–53.